The effect of cooling rate on binary nucleation

PETER P. WEGENER and K.R. SREENIVASAN

Dept. of Engineering and Applied Science, Yale University, New Haven, CT 06520, USA

Introduction

In gasdynamic flows at high temperatures, the real gas effects that occur can be treated by equilibrium thermodynamics provided the ratio of the time scale of the flow to that required to establish a new thermodynamic state is large. However, at high supersonic and hypersonic speeds, the time-scale ratio becomes comparable to unity, and departures from thermodynamic equilibrium set in. The equilibrium is restored only after a characteristic period called the relaxation time. At increasing speeds – or temperatures – typical relaxation processes are those of vibrational excitation, dissociation, ionization, etc. of the gas. In such flows – even if thermodynamic equilibrium is maintained – the phenomenon of acoustic dispersion occurs with the speed of sound depending on frequency.

During his time at Delft, L.J.F. Broer made major contributions to this field. In 1951 [4] he was the first to treat the theory of acoustic relaxation due to heat capacity lag in compressible flows. Independently of other work [3, 7, 13, 22], he was also responsible [5] for clarifying some confusion that arose with the appearance of additional papers in the intervening period. Finally, while at Eindhoven, he summarized the field from the retrospective views of a physicist [6]. In his papers, Broer derived expressions for the high and low frequency limits of the acoustic velocity, and showed independently that in the dynamics of compressible flows with relaxation, the characteristics of this type of flow are determined by the high-frequency limit of the speed of sound. This seemingly puzzling fact was later verified experimentally in supersonic flow of a dissociating gas mixture in thermodynamic equilibrium [20].

Restricting ourselves to relaxing flows with a single non-equilibrium mode whose instantaneous state is characterized by a progress variable q, the general approach is to introduce a rate equation

$$\frac{Dq}{Dt} = \frac{F(p, \rho, q)}{\nu} \tag{1}$$

in addition to the equations of motion and state. Here ν is an internal time scale and the relaxation function, F, has the property that

$$F[p, \rho; \bar{q}(p, \rho)] = 0 \tag{2}$$

in thermodynamic equilibrium where $q = \bar{q}$ and $\nu = 0$. Typically in dissociating flow, $\bar{q}(p, \rho)$ is the law of mass action. Finally a relaxation time, τ, can be defined by

$$\tau = -(\partial F/\partial q)^{-1}. \tag{3}$$

Many nonequilibrium problems in flows have now been solved using these equations, often with equation (1) linearized about the equilibrium state.

Normally, the limiting sound speeds in nonequilibrium flow – usually called the frozen and equilibrium sound speeds in gasdynamics – are numerically not too different from each other. A striking exception to this generalization is provided by nonequilibrium flow with condensation. Here, in a rapid expansion a vapor becomes supersaturated and at some thermodynamic state an irreversible collapse of the supersaturated conditions leads to equilibrium. Droplets (or solid particles) appear and the limiting sound speeds in this mixture may differ substantially (e.g. [19]). In fact owing to the heat of vaporization, condensing flows – especially water – exhibit strong effects of departure from perfect gas flows. However, our knowledge of the rates of the condensation process based on first principles is far from being complete. Therefore we must base calculations of flow fields on empirical boundary conditions. In keeping with the general approach outlined above, in condensation studies one defines the progress variable of a single condensing vapor – ordinarily carried at small mole fraction in a non-condensing gas – by $q \equiv g = m_c/m$, the mass fraction of the condensate. If a flow process such as an isentropic expansion proceeds into the coexistence region without condensation, the vapor partial pressure p_v exceeds the saturation pressure p_∞, and the saturation ratio $p_v/p_\infty > 1$. (In other words the relative humidity exceeds 100%.) At some state condensation commences and after equilibrium is established $g = \bar{g}$ where $\bar{g}(p, \rho)$ is given by the Clausius-Clapeyron equation. During the nonequilibrium state, we have $0 < g < \bar{g}$. Two separate relaxation times can be defined here. Firstly, a certain time elapses during which a gas sample moves from the saturated state to that of the onset of condensation. Secondly, we can count the time of actual condensation from its onset to the instant that some fraction of the final equilibrium state, say $g = (1/e)\bar{g}$, is attained. With these two relaxation times obtained from experiment, and using the linearized form of equation (1), Bartlmä [2] computed the structure of two-dimensional supersonic nozzle flows with water vapor condensation in air. He employed the method of characteristics as prescribed by Broer and achieved remarkable agreement with the experiment.

Unfortunately, however, the theory of homogeneous and binary nucleation of vapors in the supersaturated state (see later) does not permit the formulation of a viable rate equation based on first principles: for this reason empirical data are needed, typically in the form of relaxation times. This can

be obtained from a knowledge of the supersaturation. A convenient way of expressing the supersaturation is in terms of the adiabatic supercooling, ΔT_{ad} given by

$$\Delta T_{ad} = T_s - T_k, \tag{4}$$

where T_s is the saturation temperature and T_k the temperature at the onset of condensation, both determined on an isentrope. This expression is useful for the representation of experimental data since small errors in temperature may lead to large errors in the supersaturation p_v/p_∞ owing to the exponential dependence of vapor pressure on temperature. Empirically it has been found (for references and an extended discussion see e.g. [19]) that the adiabatic supercooling is a function of the initial saturation ratio (or relative humidity, ϕ_i) and the average cooling rate in the flow process,

$$\Delta T_{ad} = f(\phi_i, -\mathrm{d}T/\mathrm{d}t). \tag{5}$$

Once this function is known, the relaxation times of the process may be determined for insertion into the semi-empirical rate equation.

We shall here be concerned with new experimental results on the condensation of binary systems, i.e. mixtures in which two vapors condense simultaneously and shall restrict ourselves to the determination of empirical results described by equations (4) and (5).

Experimental methods

Experiments on homogeneous and binary nucleation were carried out in a shock tube. A shock tube consists of two sections of pipe – the driver and the driven section – that are separated by a diaphragm. The two sections are initially filled with the same gas at the same temperature, with the pressure in the driver section higher than that in the driven section. Upon breaking the diaphragm, a nominally one-dimensional, unsteady flow system is set up in the tube as shown schematically in Figure 1 which also includes designations for flow regimes. A shock wave at the shock Mach number $M_s = u_s/a_1$ (where u_s is the speed of the shock in the stationary frame of reference and a_1 is the speed of sound in region 1) travels to the right. An expansion wave travels to the left at a front speed a_4 and is followed by an expansion fan that sets the gas initially at rest in region 4 in motion to the right. A contact surface – an entropy discontinuity separating the cold outflow air of the expansion from the shock-heated air on the right – divides the gas samples initially in either region of the tube. In Figure 1 a distance–time (or x–t) diagram is shown at the top and particle paths of gas samples are indicated. Below the x–t-diagram are shown instantaneous pressure and temperature distributions in the flow system at time t_1, as well as the corresponding flow regimes in the tube itself.

We particularly note the cooling of the gas in the expansion fan between

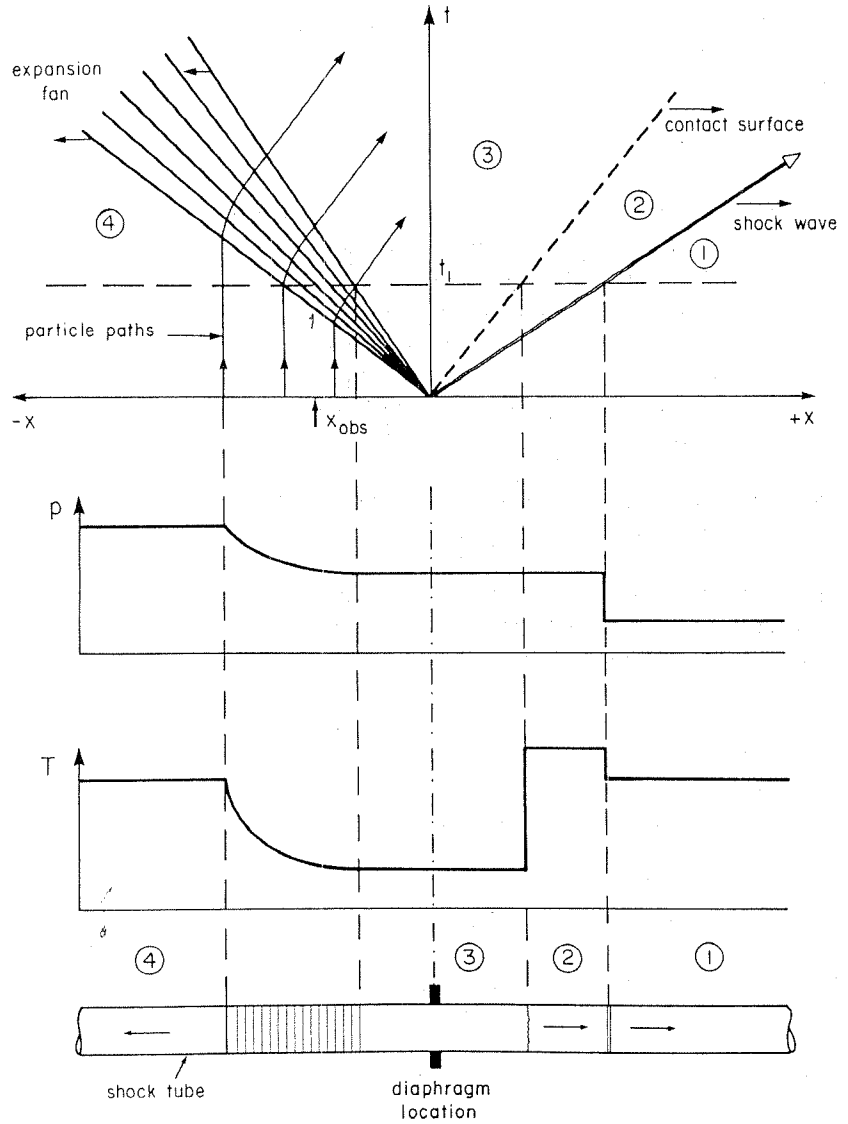

Figure 1. Schematic $x-t$-diagram of shock tube flow of an ideal gas (top). Flow structure at a given instant t_1 assuming a constant initial temperature in the shock tube (bottom)

regions 4 and 3. It is this cooling which makes the shock tube a useful device for condensation studies: small amounts of condensing vapor or vapors added to the carrier gas in the driver section will condense due to this cooling. If condensation occurs in the expansion, the heat addition to the flow owing to the latent heat of the small amount of condensate will remain negligible. Consequently, the ideal shock tube operation (e.g. [11]) as shown in Figure 1

remains unaffected. With the ratios of the specific heats $\gamma_1 = \gamma_4$, and $a_1 = a_4$ (i.e. $T_1 = T_4$) we find the main shock tube operating equation

$$\frac{p_4}{p_1} = \frac{p_2}{p_1}\left[1 - \frac{(\gamma-1)(p_2/p_1 - 1)}{\sqrt{(2\gamma)}\sqrt{(2\gamma + (\gamma+1)(p_2/p_1 - 1))}}\right]^{-2\gamma/\gamma-1}, \quad (6)$$

where p_2/p_1, the pressure ratio across the shock wave, is given by

$$\frac{p_2}{p_1} = \frac{2\gamma M_s^2 - (\gamma - 1)}{\gamma + 1}. \quad (7)$$

Since $p_2 = p_3$ in the flow system, and since the unsteady expansion fan is isentropic, pressure and temperature in region 3 are given by Poisson's law

$$\frac{T_3}{T_4} = \left(\frac{p_3}{p_4}\right)^{(\gamma-1)/\gamma} = \left(\frac{p_2/p_1}{p_4/p_1}\right)^{(\gamma-1)/\gamma} \quad (8)$$

How realistic are these assumptions in actual flow systems? For one, at the high Reynolds numbers of interest here viscous effects are in fact negligible in the bulk of the flow. However, the postulated ideal expansion fan requires instantaneous diaphragm breakage and the resulting infinite initial acceleration of the flow system as shown in Figure 1. In real flows careful measurements at our laboratory by Lee [10] of the pressure–time function in expansion fans have shown the limitation of this assumption. It was found that shortly after diaphragm breakage the lines of equal temperature and pressure in the expansion – the so-called characteristics† – are in fact straight lines. However, owing to the finite acceleration of the flow system, the origin of the characteristics – or the origin of the expansion fan – is not seen at the point $x = t = 0$. Rather, the actual situation can be explained by a slightly displaced fan origin location to a point below (i.e., slightly negative t) and to the right (i.e., slightly positive x) of the ideal origin. This point has been named the 'virtual origin' of the expansion fan and the resulting small empirical correction may be applied to the experiments.

Return to Figure 1. Upon arrival of the head of the expansion fan, the pressure and temperature drop simultaneously at the observation station and they are related by equation (8). This process is not unlike that of steady nozzle flow viewed in the Lagrangian sense or the expansion in a Wilson cloud chamber. At some known time at some location condensation will appear as determined with a photomultiplier tube by laser light scattered from the cloud of droplets. The pressure history is measured with a piezo-electric pressure transducer of a short response time. Consequently the corresponding temperature can be computed. However, the vapor sample whose state at the

† Characteristics are known from the theory of hyperbolic partial differential equations. These straight lines (Figure 1, top) are lines of constant thermodynamic states and flow speed.

onset of condensation is not known, undergoes a thermodynamic time history different from that followed at the observation station. As indicated graphically by particle paths in the x–t-diagram at the top of Figure 1, the history of the particle (or gas sample) set into motion by the expansion fan at $t = t_0$ is computed by

$$x = -\frac{a_4 t}{\gamma - 1}\left[2 - (\gamma - 1)\left(\frac{t_0}{t}\right)^{(\gamma-1)/(\gamma+1)}\right]. \tag{9}$$

Observations at a fixed location as a function of time can therefore readily be transformed by equation (9) to the paths actually undergone by the gas samples using the equations given. The cooling rate entering equation (5) can be computed from the foregoing and it is given by

$$\frac{dT}{dt} = -\frac{2T_4}{t}\frac{\gamma - 1}{\gamma + 1}\left[\frac{x}{a_4 t} - \frac{2(x/a_4 t + 1)}{\gamma + 1}\right]^2. \tag{10}$$

The experiments to be described here were carried out with techniques developed at our laboratory (e.g. [1, 10]). However, a plastic shock tube with an internal diameter of 2.5 cm was used. For binary nucleation studies, a mixing station was developed to fill the driver section of the shock tube with a well defined mixture of ethanol/water and carrier gas (N_2 or A). High purity carrier gases were used together with reagent type ethanol and distilled water. The light scattering viewing station was moved from locations close to the diaphragm (high cooling rates, Figure 1) to about one meter into the driver section. The light scattering signal – if any – was recorded simultaneously with the pressure history measured at $x = -61$ cm. The onset of condensation was noted as a steep increase in the photomultiplier output beyond the background light signal including electronic noise. By triggering the photomultiplier output by the pressure signal corresponding to the arrival of the head of the expansion fan at $x = -61$ cm, the time at which condensation occurs can be calculated. With this set-up, the minimum detectable condensation mass fraction is estimated to be $g \simeq 10^{-3}$. Consequently, the abiabatic supercooling and the condensation onset temperatures are known to an accuracy of about ± 2°C.

Experimental results

(a) Ethanol in nitrogen; homogeneous nucleation

To check our methods, a set of experiments were performed with ethanol condensing by homogeneous nucleation in nitrogen since previous nozzle experiments [21] are available for comparision. Experiments to determine the onset of condensation as a function of distance from the diaphragm in the driver section – i.e. the cooling rate – were performed. For all ethanol

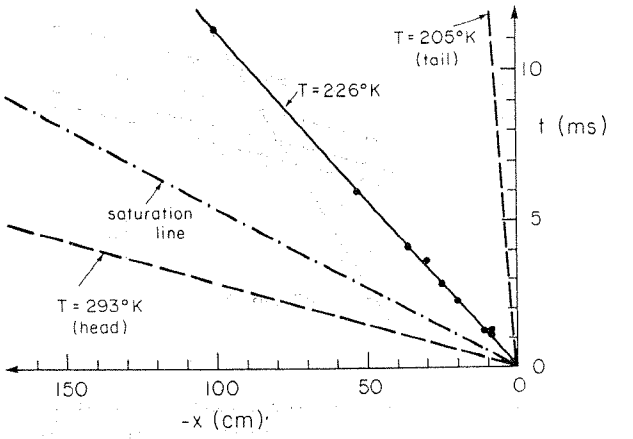

Figure 2. Onset of condensation of ethanol in nitrogen in the expansion fan of a shock tube as a function of upstream distance from the diaphragm. Note that the experimental points (•) obtained at different distances from the diaphragm lie close to the $T = 266$°K characteristic indicating small cooling rate effects. For experimental conditions see the text

experiments $p_4 = 1{,}350$ torr (1.78 atm) with the ethanol partial pressure $(p_4)_{eth} = 3$ torr at $T_4 = 293$°K and $p_4/p_1 = 10$. Figure 2 is patterned after the top sketch of Figure 1. Irrespective of the location of the observation station, the results scatter around the $T = 226$°K characteristic. The characteristic of the saturation temperature is also given and it is computed from the vapor pressure equation

$$\log p_\infty(\text{torr}) = -\frac{2371}{T(°\text{K})} + 9.76, \tag{11}$$

valid for $219 < T < 277$°K (for references see [21]).

The shock tube results of Figure 2 are compared with the steady-state nozzle experiments in Figure 3. The initial states and the states at the onset of condensation are here given in the traditional pressure – temperature diagram. We note excellent agreement of the results obtained with these two different gasdynamic methods.

Finally, we can compute the adiabatic supercooling as a function of cooling rate from equations (8) and (10) for the shock tube data. The same function can be obtained for the nozzle experiments and the combined results are shown in Figure 4. Although the cooling rates differ roughly by a factor of 200, no substantial changes are noted in the adiabatic supercooling. The implication is clearly that the function f in equation (5) is essentially indeindependent of $-dT/dt$ for the range considered here.

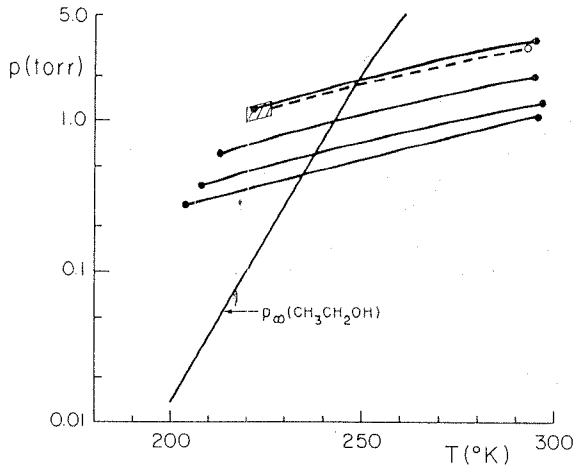

Figure 3. Condensation of ethanol in nitrogen by homogeneous nucleation in the supersaturated state. Condensation in the expansion fan of the shock tube on an isentrope (shaded area) with the initial state (open circle) given in the text. Solid points indicate condensation observations in steady flow in the supersonic nozzle (from Table II [21]). For both experimental methods condensation was observed by laser light scattering

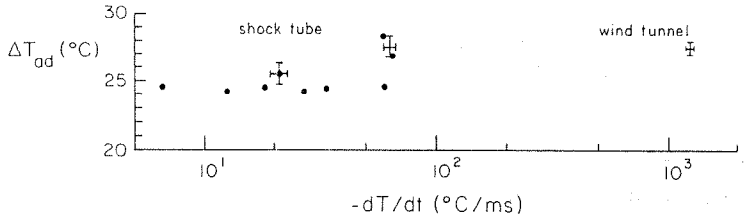

Figure 4. The adiabatic supercooling, equation (4), of ethanol in nitrogen as a function of cooling rate in the shock tube (this work) and the supersonic nozzle [21] obtained from the results of Figures 2 and 3

(b) Ethanol and water in nitrogen: binary nucleation

Two independent series of experiments on binary nucleation were carried out in the shock tube using the same equipment. The constant experimental conditions were as follows.

Carrier gas: high purity nitrogen (99.998% pure)

$$T_4 = 293°\text{K}; p_4 = 1{,}350 \text{ torr} = 1.78 \text{ atm}$$

$$(p_4)_{\text{eth}} = (p_4)_{H_2O} = 6.70 \text{ torr} = 8.82 \times 10^{-3} \text{ atm}$$

$$x_{\text{eth}} = x_{H_2O} = 0.0050$$

$$p_4/p_1 = 10; \gamma = 1.40; M_s \simeq 1.6$$

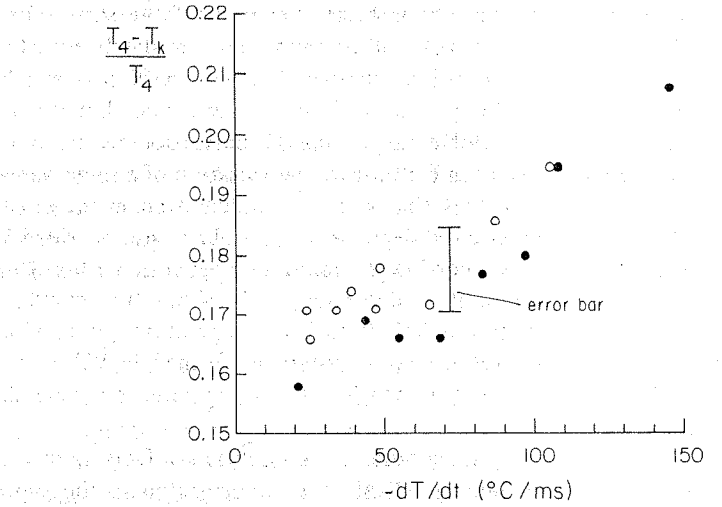

Figure 5. Dimensionless temperature at the onset of binary nucleation (T_k) as a function of cooling rate for the conditions of Figure 3. Note that larger values of $(T_4 - T_k)/T_4$ – i.e. lower values of T_k for T_4 = const – denote a larger supercooling. The two symbols denote two series of experiments taken separately at identical conditions

During the experiments the condensation onset was measured with the photomultiplier location varying from -70 cm to -6 cm in the driver section with respect to the diaphragm station at $x = 0$. In contrast to the results of Figure 2, this time the onset states of condensation were not located on one characteristic. In fact close to the diaphragm (high cooling rates), the condensation onset deviated to lower temperatures.

The adiabatic supercooling cannot be computed readily for binary nucleation since the equivalent expression of the saturated vapor pressure in a binary mixture must be determined separately for each thermodynamic state through which the mixture passes. In fact the mixture departs markedly from the ideal state and empirical relations for the activity coefficients must be considered. For this reason the results are shown in Figure 5 in the form of a dimensionless temperature at the onset of condensation as a function of cooling rate with the latter computed as discussed before. We now note a strong cooling rate effect which clearly exceeds the scatter of the data. However, at cooling rates below $-dT/dt \leqslant 50°\text{C/ms}$ the thermodynamic state at the onset of condensation seems to be little dependent on the cooling rate.

Discussion and conclusions

In this work the shock tube is again shown to be a useful tool in condensation studies. In particular the method readily permits operation at the low

temperatures of interest in the atmospheric chemistry of the stratosphere toward which our experiments with other vapors are ultimately directed. Results on condensation of ethanol in nitrogen agree well with prior steady-state supersonic nozzle data. As previously found for water condensation in air [15, 19] the effect of the cooling rate on the adiabatic supercooling is not pronounced in the range tested. In contrast to condensation of a single vapor, it is found for the first time that the onset of condensation in the binary water/ethanol system in nitrogen is dependent on cooling rate, provided its values are $-\mathrm{d}T/\mathrm{d}t \gtrsim 50^\circ\mathrm{C/ms}$. For lower cooling rate again no strong effect is seen. This latter fact permits the comparison of the shock tube results at the low cooling rates with extrapolations to low temperatures of previous experimental work on the water/ethanol system performed in Wilson and diffusion cloud chambers [9, 12] in which the cooling rates are generally much lower.

We recall that in contrast to some other non-equilibrium effects no quantitative theory exists for expressing reliably the condensation in the supersaturated state in the form of equation (5). Our qualitative understanding is based on the theory of homogeneous nucleation [17, 18, 23, 24] as extended to binary systems [9, 14]. In these theories condensation in the supersaturated state is treated in the absence of foreign aerosols. Droplets of a critical size – called nuclei – given by the well-known expressions of Gibbs, Kelvin and of Helmholtz are formed by fluctuations in the supersaturated state, and the energy of their formation in terms of the Gibbs free enthalpy is given by ΔG^*. By deriving a kinetic frequency factor, K, the rate of nucleation, J, of surviving droplets, i.e. the number of nuclei formed per unit volume and time at a fixed supersaturated state is given by

$$J = K \exp(-\Delta G^*/kT). \tag{12}$$

In a typical experiment the expansion proceeds past the equilibrium vapor pressure curve to supersaturated states (Figure 3) until the nucleation rate computed by equation (12) rises steeply and condensation sets in. In the Lagrangian view, the time of flight from saturation to the precipitous onset of condensation corresponds to the first of the two relaxation times discussed previously. It is this relaxation time that is implicit in the data of condensation onset states shown in this paper.

Why does the cooling rate affect binary nucleation more prominently† as seen from Figures 4 and 5? Some speculation on this point will conclude our remarks. The energy of droplet formation in homogeneous and binary nucleation is strongly dependent on the surface tension of the droplets, σ. An inspection of the actual expression for ΔG^* shows that $\Delta G^* \sim \sigma^3$, i.e. the

†For ethanol nucleation (Figure 4) the supercooling changes by at most 4°C for an increase in cooling rate by a factor of about 200. In ethanol/water nucleation (Figure 5), the temperature at the onset of condensation decreases by about 15°C for an increase in cooling rate by a factor of only about 7.

surface tension enters as the exponent raised to the third power in equation (12). Clearly, then, the surface tension must be well known for quantitative predictions. However, bulk surface tension is not known as a function of temperature near the states of condensation of Figures 4 and 5. As has long been known, there is in addition a possible dependence of surface tension on droplet radius in single liquids [23, 24]. The first Monte Carlo calculations on the same effect for binary liquids [16] appear to show that small clusters containing only a few molecules exhibit surface tensions *below* that of the bulk at the same temperature. Finally it is well known that the book values of surface tension of binary liquids refer to thermodynamic equilibrium. Here the flat liquid surface is known to be enriched in the component of the lower surface tension (in our situation the ethanol). With the high fluxes of evaporating and condensing molecules near the size of the critical nucleus, it is likely that no equilibrium value of surface tension – as given in handbook tables – is established. In turn the effective surface tension in this dynamic situation will be *higher* than the book values with more water molecules at the surface than at equilibrium with its concentration gradients. This strong surface tension dependence discussed above predicts a delay of condensation if in fact the actual surface tension were higher than its equilibrium value. Mirabel and Katz (see Fig. 8 in [12]) were able to force agreement of theory and diffusion cloud-chamber condensation experiments on the same system by inserting surface tension values higher than those found in tables. This effect – if present – ought to be most noticeable at small mole fractions of ethanol in water, the mixture region of the rapid drop of surface tension with change of composition. Unfortunately, at our low temperatures of condensation, not even equilibrium surface tension data exist. At any rate, at higher cooling rates, higher effective surface tension values of the forming droplets would delay condensation. Qualitatively the results of Figure 5 could therefore be explained.

Much of this reasoning may however be faulty if the concept of concentration gradients breaks down for the very small drops expected in our experiments [8]. There is simply not enough droplet surface to sufficiently place molecules in any pattern predictable from the continuum of Gibbs' adsorption theory or in patterns to be expected at high cooling rates. In sum, we are at present unable to explain the observed effect of cooling rate on supercooling in binary nucleation.

Acknowledgement

Discussions with Dr. P. Mirabel, Chemistry, University of Strasbourg and Dr. F. Peters of Yale University are gratefully acknowledged. The work was supported by Grant NAG-2-15 of the Ames Research Laboratory of the National Aeronautics and Space Administration to Yale University.

References

1. Barschdorff D (1975) Phys Fluids 18: 529.
2. Bartlmä F (1963) Z Flugwiss 11: 160.
3. Brinkley SR Jr and Richardson J (1953) Fourth Symposium (International) on Combustion, p. 450. The Williams & Wilkins Co., Baltimore, Md.
4. Broer LJF (1951) Appl. Sci. Res A2: 477.
5. Broer LJF (1958) J Fluid Mech 4: 276.
6. Broer LJF (1970) 'Some Basic Properties of Relaxation Gasdynamics', pp. 2–31, Nonequilibrium Flows, Part II in Gasdynamics, Vol. 1 (ed Peter P Wegener). Marcel Dekker, Inc., N.Y.
7. Chu BT (1958) Proc Heat Transf & Fluid Mech Inst 80.
8. Flagoellet C, Dinh Cao M, and Mirabel P (1980) J Chem Phys 72: 544.
9. Flood H (1934) Z Phys Chem A170: 286.
10. Lee CF (1977) Condensation of H_2O and D_2O in Argon in the Centered Expansion Wave in a Shock Tube, 1977 Joint Applied Mechanics, Fluids Engineering and Bioengineering Conference. Yale University, New Haven, CT June 15–17, ASME, N.Y.
11. Liepmann HW and Roshko A (1957) 'Elements of Gasdynamics'. Wiley, N.Y.
12. Mirabel P and Katz JL (1977) J Chem Phys 67: 1697.
13. Moore FK (1958) J Aero Space Sci 25: 279.
14. Reiss H (1950) J Chem Phys 18: 840.
15. Smith LT (1971) AIAA J 9: 2035.
16. Stauffer D, Binder K and Wildpaner V (1974) Water, Air and Soil Pollution 3: 515.
17. Volmer M and Weber A (1926) Z Phys Chem 119: 277.
18. Volmer M (1939) 'Kinetik der Phasenbildung'. Steinkopff, Leipzig.
19. Wegener PP (1975) Acta Mechanica 21: 65.
20. Wegener PP and Cole JD (1962) Eighth Symposium (International) on Combustion, p. 348. The Williams and Wilkins Co., Baltimore, Md.
21. Wegener PP, Clumpner JA and Wu BJC (1972) Phys Fluids 15: 1869.
22. Wood WW and Kirkwood JG (1957) J Appl Phys 28: 395.
23. Zettlemoyer AC (1969) (ed) 'Nucleation'. Marcel Dekker, N.Y.
24. Zettlemoyer AC (1977) 'Nucleation Phenomena'. Elsevier, N.Y.